# A Series Slot Array Antenna for 45°-Inclined Linear Polarization With SIW Technology

Dong-yeon Kim, Woo-Sung Chung, Chang-Hyun Park, Sang-Joo Lee, and Sangwook Nam, *Member, IEEE*

***Abstract*—The design method for a standing-wave series slot array antenna with 45°-inclined linear polarization in the Ka-band is presented. The proposed $16 \times 8$ planar slot array antenna consisted of arrays with alternating reactance slot pairs that could achieve impedance matching and uniform field excitation, simultaneously. Furthermore, the grating lobes were effectively suppressed with the help of these radiating units due to the one-half guided wavelength slot spacing. An equivalent circuit analysis was done to evaluate the input impedances of the radiating and feeding lines with the impedance recursive formulas as well as the mode voltages of the radiating slot elements. In addition, a wideband transition with a 30.13% bandwidth under the criteria of less than VSWR 1.5:1 was presented to provide the necessary power with the minimal reflection and to prevent the distortion of the radiation patterns. The proposed planar slot array antenna occupied an aperture area of $57.4 \times 51.6$ mm. The measured bandwidth, gain, and efficiency were 990 MHz (2.88%), 24.3 dBi, and 53.7%, respectively. Furthermore, the side lobe levels (SLLs) were verified for each cutting plane with $-13.57$ dB and $-13.17$ dB, respectively. The proposed antenna structure was achieved with a substrate integrated waveguide (SIW) with the low costs and lightweight features.**

***Index Terms*—Alternating reactance slot pair, slot array antenna, substrate integrated waveguide (SIW) technology.**

## I. Introduction

WAVEGUIDE (WG)-FED slot array antennas are widely used for many millimeter-wave communication systems due to their electrical and physical advantages such as high gain, efficiency, and low-profile. Especially in many radar systems like collision avoidance automotive radar, monopulse radar, and synthesis aperture radar (SAR), the WG-fed slot array antennas are promising candidates for accurate beam forming as well as low side lobe levels (SLLs). Furthermore, these antennas can be used for high-speed wireless communication and direct broadcast satellite (DBS) systems requiring specific linear or circular polarization (LP or CP) [1], [2].

Over the past few decades, conventional WG-fed shunt slot array antennas have been designed with well-established design equations, which take into consideration both internal and external coupling effects [3]. The series slot array antennas also have been investigated and analyzed by Orefice and Elliott oriented parallel to the shunt slot array design procedure [4]. Both the shunt and series slot array elements are cut on the upper rectangular waveguide (RWG) broad wall with a slot spacing of one-half guided wavelength at the operating frequency. In order to generate in-phase electric field distributions on every radiating slot, alternating offsets and tilt angles should be adopted for WG-fed shunt and series slot array antennas, respectively.

Meanwhile, in some specific radar applications such as collision avoidance automotive radar systems, a 45°-inclined LP is required to alleviate the interference coming from the opposite direction. It is difficult to generate an arbitrary polarization using fundamental shunt and series WG-fed slot array antennas, which generate only the vertical or horizontal LP. Furthermore, the element spacing of a guided wavelength is inevitable for the in-phase electric field distribution of 45°-inclined series slot array elements, which consist of the resonant slot length only [4]. As a result, the grating lobes can easily occur in the longitudinal direction of the radiating lines and the radiation efficiency will be decreased. Besides, as the tilt angle of a centered-inclined series slot increases, the corresponding self-impedance also increases, and eventually, the maximum self-resistance appears when the tilt angle reaches 45° [5]. In other words, the number of series connected slot elements for an arbitrary LP should be restricted for impedance matching to the input wave impedance of a given air-filled WG.

Various slot array antennas have been proposed for the 45°-inclined LP with different operating mechanisms for the traveling-wave excitation [6]–[8]. The post-wall WG-fed parallel plate slot array antenna was designed with two reflection-cancelling slots and a main radiating slot to generate a 45°-inclined LP [6]. In addition, to minimize the reflection, which can occur from the radiating elements, reflection-cancelling inductive posts located on each radiating slot with the proper spacing were introduced [7]. In addition, the traveling-wave-fed slot array antenna that has open-ended circular cavities surrounding each series of slots etched on the narrow wall of the radiating WGs is presented in [8]. The posts under every radiating slot contribute to the coupling amount to the air boundary by means of their location and height. Nevertheless, these traveling-wave-fed slot array antennas, which adopt the end-fed structure, are susceptible to beam tilting for frequency variation as well as asymmetric radiation patterns.

This paper presents a new design method and analyzes with equivalent circuit models the standing-wave-fed series

Manuscript received July 11, 2011; revised September 03, 2011; accepted October 10, 2011. Date of publication February 03, 2012; date of current version April 06, 2012. This work was supported by the LIG Nex1 Co., Ltd.

D.-Y. Kim and S. Nam are with the Institute of New Media Communication (INMC), School of Electrical Engineering and Computer Science, Seoul National University, Seoul 151-742, Korea (e-mail: dykim@ael.snu.ac.kr).

W. Chung, C.-H. Park and S.-J. Lee are with the ISR R&D Laboratory, LIG Nex1 Co., Ltd., Yongin-si 446-798, Korea (e-mail: changhyun.park@lignex1.com).

Color versions of one or more of the figures in this paper are available online at http://ieeexplore.ieee.org.

Digital Object Identifier 10.1109/TAP.2012.2186270

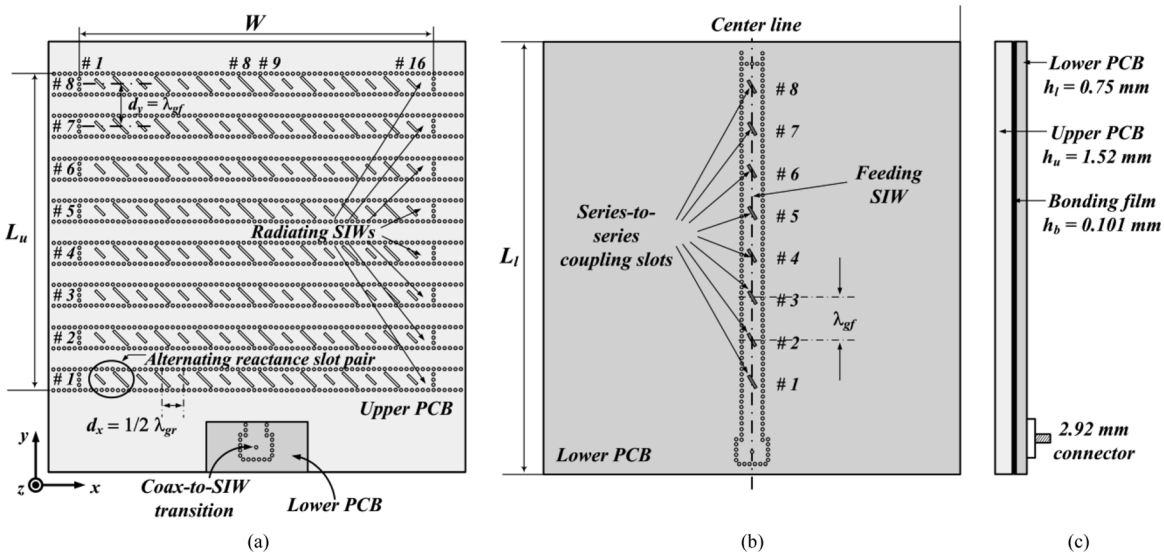


Fig. 1. The proposed antenna geometry. (a) Top view. (b) The feeding structure that has series-to-series coupling slot arrays. (c) Lateral view.

slot array antenna generating a 45°-inclined LP. We proposed an alternating reactance slot pair for a radiating unit that has both an inductive and a capacitive reactance with relative low resistance to design the element arrangement with one-half guided wavelength slot spacing. Furthermore, the proposed antenna was realized through substrate integrated waveguide (SIW) technology with low costs and lightweight features. In Section II, the proposed antenna configuration will be described. In addition, the detailed design method for the SIW transmission line, alternating reactance slot pair, and grating lobe suppression will follow in Section III. Furthermore, equivalent circuit analysis was done for a linear and planar slot array antenna as well as the dual-resonant coax-to-SIW transition. Finally, in Section IV, the electrical performance of the proposed antenna will be presented with full-wave simulation and experimental results to verify the validity of the design method.

## II. Antenna Configuration

As described in Fig. 1(a), the centered-inclined series slot arrays are etched on the upper broad wall of the radiating SIWs along the center line to generate a 45°-inclined LP [11]. Every radiating slot is designed to acquire the bore sight main beam through an in-phase and uniform field distribution. Beam tilting also can be easily avoided by the center-fed method with series-to-series coupling slots as shown in Fig. 1(b). These coupling slots are etched on the bottom and top metal plates of the upper and lower PCBs (printed circuit boards), respectively, and aligned with each other precisely. Each radiating SIWs have sixteen 45°-inclined radiating elements with the precise spacing of one-half guided wavelength ($d_x = \lambda_{\rm gr}/2$) not to exceed a wavelength ($\lambda_0$) in free space. On this occasion, shorter and longer lengths of slots rather than a resonant one are arranged alternatively and periodically. The operating principle of the above alternating reactance slot pairs is clarified in Section III-B in detail. In addition, all series-to-series coupling slots are separated from each other with a guided wavelength ($d_y = \lambda_{\rm rf}$) of a feeding SIW with an equal tilt angle referenced from the center line to provide power with in-phase and equal amplitude.

The proposed antenna was designed with the SIW technology, which can be used in general PCBs with the standard process such as via holes. Radiating and feeding SIWs are inserted in the RO3035 substrates with a dielectric constant of 3.5, a loss tangent of 0.0018, and a thickness of 1.52 mm ($h_u$) and 0.75 mm ($h_l$), respectively, as shown in Fig. 1(c) for the lateral view. The upper and lower PCBs were adhered to each other with a RO4450B bonding film with a dielectric constant of 3.3, a tangent loss of 0.004, and a thickness ($h_b$) of 0.101 mm. Furthermore, the selected PCBs had the thinnest metal cladding of 17 $\mu$m to minimize undesired phase variation from the thickness of the metal plates.

## III. Design Method and Equivalent Circuit Analysis

The aperture field distribution is realized with alternating reactance slot pairs and series-to-series coupling slots located in the radiating SIWs and a feeding SIW, respectively. To suppress the grating lobes in the radiation patterns, the coordinate system of radiating elements should be taken into consideration and reflected in the design of the SIW transmission line. In addition, a wideband coax-to-SIW transition is presented and investigated with an equivalent circuit model and simulation results.

### A. SIW Transmission Line Design

As shown in Fig. 2(a), the SIW transmission line can be embedded in a general PCB connecting the top and bottom metal plates with metalized via arrays acting as a perfect electric wall (PEW) like a RWG. The width ($w$) of a radiating SIW, the diameter ($d$), and the spacing ($s$) of vias are the critical design parameters for the transmission characteristics of a SIW such as the cut-off frequency and attenuations for a fundamental $\rm TE_{10}$ mode. In order to determine the above design parameters for the operating frequency, 35 GHz in the Ka-band, it is desirable to set the operating frequency in the middle of the cut-off frequencies for the $\rm TE_{10}$ and $\rm TE_{20}$ modes. When the SIW transmission line

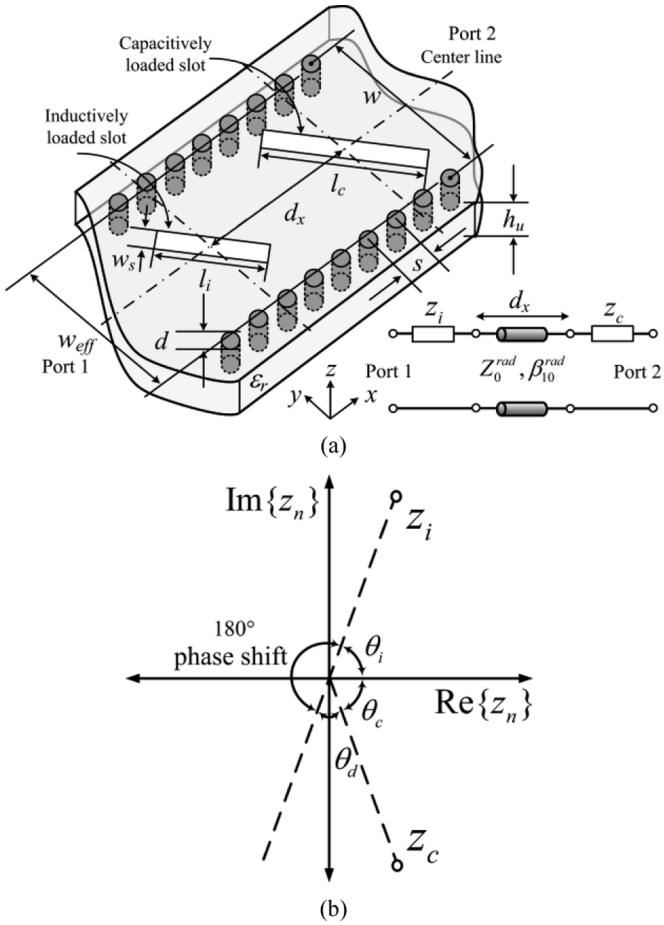


Fig. 2. The proposed alternating reactance slot pair etched on the broad wall of a radiating SIW. (a) Structure and its equivalent circuit, where $Z_0^{rad}$ is the wave impedance and $\beta_{10}^{rad}$ is the propagation constant of the $\mathrm{TE}_{10}$ mode. (b) The phase difference between the normalized self-impedances ($z_c$ and $z_i$) of an alternating reactance slot pair.

is identified with the equivalent RWG, the cut-off frequency of the $\mathrm{TE}_{10}$ mode is defined by

$$f_{c,TE10} = \frac{c}{2\pi\sqrt{\varepsilon_r}} \cdot \frac{\pi}{w_{eff}} \tag{1}$$

and the effective width of the SIW transmission line can be obtained by

$$w_{eff} = w - 1.08 \cdot \frac{d^2}{s} + 0.1 \cdot \frac{d^2}{w} \tag{2}$$

where $c$ and $\varepsilon_r$ are the light velocity and the dielectric constant of a PCB, respectively [9]. Furthermore, radiation, conduction, and dielectric losses should be reduced according to the design principle for the operating frequency. To minimize these losses, the diameter of via was chosen with the following design role [9]:

$$\frac{s}{2.5} < d < \frac{w}{8}. \tag{3}$$

Besides, the width of the SIW transmission line should be determined taking into consideration the coordinate system of the radiating elements ($d_x$ and $d_y$ in Fig. 1(a)) so as not to generate the grating lobes in both the $yz$ and $zx$ cutting planes. As shown in Fig. 2(a), the SIW transmission line consisted of via arrays with a diameter and spacing of 0.4 mm and 0.7 mm for the via. When the width of the radiating SIW was chosen as 3.44 mm, a cut-off frequency and slot spacing for the $\mathrm{TE}_{10}$ mode of 25.06 GHz and 3.34 mm ($= 0.4 \cdot \lambda_0$), respectively, was obtained.

### *B. Alternating Reactance Slot Pair*

The most important process in a 45°-inclined series slot array antenna design is the impedance extraction of a single slot module. As done in [10], the interpolated self-impedance of the resonant slot with a slot width ($w_s$) of 0.4 mm has a real high resistance of $4.67 \cdot Z_0^{rad}$. As a result, it is hard to match the input impedance of a 45°-inclined series slot array antenna to the wave impedance of a given radiating SIW ($Z_0^{rad}$) without any matching circuits. Therefore, the conventional WG-fed series slot array antenna presented in [4] with its impedance matching and bore sight main beam are infeasible with only 45°-inclined resonant radiating slots due to their high input impedances and out-of-phase slot mode voltages, respectively.

For that reason, the alternating reactance slot pairs were proposed as depicted in Fig. 2(a) comprised of shorter and longer slot lengths rather than resonant one representing inductive and capacitive load impedance, respectively [10]. The currents flowing into these series connected slots have equal amplitude and out-of-phase due to the spacing of the one-half guided wavelength transmission line at the operating frequency as shown in Fig. 2(a). Therefore, the mode voltages can be calculated with just the self-impedances of an alternating reactance slot pair as shown in Fig. 2(b). The inductive and capacitive self-impedances denoted by $z_i$ and $z_c$ that are normalized to the wave impedance of a given radiating SIW can be plotted in the complex plane with respect to the amplitude and phase. The phase of these inductive and capacitive self-impedances are then given by

$$\theta_n = \tan^{-1}\frac{\mathrm{Im}\{z_n\}}{\mathrm{Re}\{z_n\}}, n = i \; and \; c. \tag{4}$$

Besides, the phase difference of the alternating reactance slot pair separated by a half guided wavelength can also be obtained by

$$\theta_d = 180^\circ - \theta_i - |\theta_c|\,. \tag{5}$$

The normalized self-impedances of an alternating reactance slot pair were chosen as $0.123 + j0.7269$ and $0.1253 - j0.7523$, respectively, based on the linearly interpolated slot impedance data. The phase difference of the mode voltages between these slots can be calculated using (4) and (5) with 19.07°. As a result, almost in-phase electric fields can be induced in the narrow width of each radiating slot. Moreover, the amplitudes of mode voltages are also nearly the same because of the symmetric impedance property of a single series slot module [10]. In this calculation, the mutual coupling effects were not considered.

### *C. Linear Slot Array Design and Analysis*

As shown in Fig. 3, the proposed linear slot array antenna has a periodic arrangement of alternating reactance slot pairs and it is fed by a series-to-series coupling slot at the center of a radiating SIW. Furthermore, the series connected radiating slots are terminated by short-circuited SIW stubs with a half guided

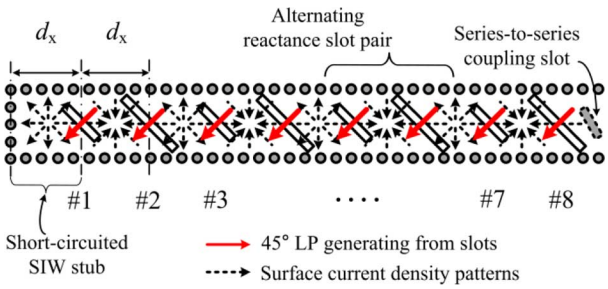


Fig. 3. The left section of a linear slot array antenna with the surface current density patterns and 45°-inclined electric fields on radiating slots.

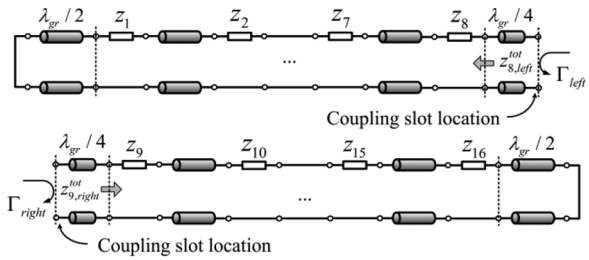


Fig. 4. The equivalent circuit of a linear slot array antenna referenced to a coupling slot location.

wavelength from the last radiating slot #1 and #16, and represent the standing-wave excitation due to the equal radiating slot spacing $(d_x)$. The surface current density patterns on the top metal plate of the radiating SIW containing the 45°-inclined series slots are depicted in Fig. 3. Although the 45°-inclined series slots generally cut the surface currents, the directions of the currents for the inductively and capacitively loaded slots are opposite to each other. Therefore, the alternating reactance slot pair has an out-of-phase current distribution. Nevertheless, the in-phase 45°-inclined electric fields can be induced due to the alternating reactance components. It was observed that the alternating reactance slot pairs act as slot offsets and alternating tilt angles of shunt and series slot array antennas, respectively, for in-phase electric field radiation [3], [4].

The proposed linear slot array antenna can be presented by the equivalent circuit with a transmission line network referenced to the coupling slot location as shown in Fig. 4. The series connected impedances $(z_n)$ stand for the self-impedances of the 45°-inclined series slot modules, which are normalized to the wave impedance of the radiating SIW. The normalized input impedance as seen from slot #8 and #9 toward the left and right sides of a radiating SIW are obtained from the following recursive impedance formulas, respectively [12].

$$z^{tot}_{n,left} = z_n + \frac{z^{tot}_{n-1} + j\tan(\beta^{rad}_{10} d_x)}{1 + j z^{tot}_{n-1}\tan(\beta^{rad}_{10} d_x)},$$
$$n = 2, 3, \ldots, 8$$
$$z^{tot}_{n,right} = z_n + \frac{z^{tot}_{n+1} + j\tan(\beta^{rad}_{10} d_x)}{1 + j z^{tot}_{n+1}\tan(\beta^{rad}_{10} d_x)},$$
$$n = 15, 14, \ldots, 9 \quad (6)$$

where

$$z^{tot}_m = z_m + j\tan(\beta^{rad}_{10} d_x), m = 1, 16 \quad (7)$$

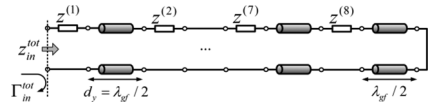


Fig. 5. The equivalent circuit of a feeding SIW.

and $\beta^{rad}_{10}$ is the propagation constant for the $\mathrm{TE}_{10}$ mode of a given radiating SIW. The reflection coefficients as seen from slot #8 and #9 toward both ends can be obtained by

$$\Gamma_{8,left} = \frac{z^{tot}_{8,left} - 1}{z^{tot}_{8,left} + 1}$$
$$\Gamma_{9,right} = \frac{z^{tot}_{9,rightt} - 1}{z^{tot}_{9,right} + 1}. \quad (8)$$

Meanwhile, the reflection coefficients to the coupling slot location can be calculated with (8) and transformed by the $\lambda_{\mathrm{gr}}/4$ length of the transmission line (in Fig. 4) as follows:

$$\Gamma_{left} = \Gamma_{8,left} \cdot e^{-j2(\beta^{rad}_{10} \cdot \lambda_{\mathrm{gr}}/4)}$$
$$\Gamma_{right} = \Gamma_{9,right} \cdot e^{-j2(\beta^{rad}_{10} \cdot \lambda_{\mathrm{gr}}/4)} \quad (9)$$

where $\lambda_{\mathrm{gr}}$ is a guided wavelength of a radiating SIW.

### D. Feeding Network Design and Analysis

A coupling slot arrangement was chosen with an equal tilt angle and with the spacing of a guided wavelength $(\lambda_{\mathrm{gf}})$ of a feeding SIW, as shown in Fig. 1(b). The distance between each radiating SIWs were set as $d_y = 2 \cdot w$. Therefore, the width $(w_f)$ of a feeding SIW can be determined by (1) to (3) with 3.38 mm to identify the guided wavelength of a feeding SIW with the spacing between the radiating SIWs.

A series-to-series coupling slot plays the role of a transformer, which converts the total input impedance of the radiating elements obtained from (6) to an arbitrary impedance according to the variation in the tilt angle and length of a coupling slot. The proposed planar slot array antenna can be simplified (Fig. 5) with a feeding SIW transmission line. The last radiating SIW is terminated with the short-circuited SIW stub of one-half guided wavelength of a feeding SIW and the total normalized input impedance of the planar slot array antenna is

$$z^{tot}_{(8)} = z_{(8)} + j\tan(\beta^{\mathrm{feed}}_{10} d_y)$$
$$z^{tot}_{(n)} = z_{(n)} + \frac{z^{tot}_{(n+1)} + j\tan(\beta^{\mathrm{feed}}_{10} d_y)}{1 + j z^{tot}_{(n+1)}\tan(\beta^{\mathrm{feed}}_{10} d_y)},$$
$$n = 7, 6, \ldots, 1 \quad (10)$$

where $\beta^{\mathrm{feed}}_{10}$ and $z_{(n)}$ are the propagation constant of the $\mathrm{TE}_{10}$ mode of a feeding SIW and the transformed normalized series impedance of the $n$th radiating SIW, respectively. The final total input impedance of a planar slot array antenna is $z^{tot}_{(1)}$.

The transformed impedance of a radiating SIW containing eight alternating reactance slot pairs can be determined by the tilt angle $(p)$ and length $(l_s)$ of the coupling slot as shown in Fig. 6. Specifically, the tilt angle and length of the coupling slot control the coupling amount and the phase, respectively. The

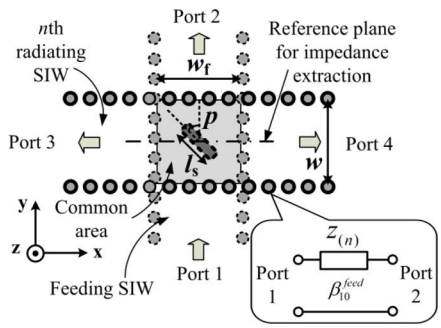


Fig. 6. The 4-port series-to-series coupling slot junction and an equivalent circuit, where $\beta_{10}^{rad}$ is the propagation constant of the $\mathrm{TE}_{10}$ mode.

series-to-series coupling slot can be modeled as an ideal transformer at the resonant frequency; however, it is hard to preserve that model at the off-resonant frequency. Therefore, an ideal transformer with a parallel resonator has been suggested to provide the exact model for a wide frequency bandwidth [13]. Meanwhile, a more accurate analysis is required for the proposed coupling junction comprised of a SIW structure and the bonding film, which has a finite thickness and a dielectric constant. As shown in Fig. 6, the input impedance of a coupling slot was evaluated when port 3 and 4 are terminated by the impedance obtained from (6), and port 2 is short-circuited at the same time. The reference plane of an input port is located in a feeding SIW just below the center of a series-to-series coupling slot (Fig. 6). The input resistance and reactance can be extracted according to the variation in design parameters with the full-wave simulator, CST MWS based on the finite-difference time-domain (FDTD) algorithm [14]. Fig. 7(a) and (b) show the results of the transformed input resistance and reactance characteristics according to the variation in the tilt angle and the half-length of a coupling slot within a range from 4° to 22° and from 1 mm to 1.3 mm, respectively. As a result, the resonant condition can be found for a single linear slot array fed by a coupling slot. The input resistance increases with the tilt angle, and pure real input impedances can be found within the range of a half-length for the coupling slot from 1.12 mm to 1.19 mm. Finally, Fig. 8 shows the resonant condition as a function of the series-to-series coupling slot parameters with linear interpolation based on the previous results of Fig. 7(a) and (b).

The calculated wave impedance $(Z_0^{\mathrm{feed}})$ of a given feeding SIW with (2) is 294.4 Ω. The design parameters of a coupling slot such as the tilt angle and half-length can be obtained from the results of Fig. 8. For uniform field distribution and impedance matching, the individual normalized impedance of a single radiating SIW series connected in a feeding SIW transmission line can be obtained as $Z_0^{\mathrm{feed}}/(n)$ where $n$ means the total number of linear slot arrays. Consequently, the tilt angle and half-length of a coupling slot were 9.87° and 1.1557 mm, respectively, for pure real input impedance $(z_{(n)} = Z_0^{\mathrm{feed}}/8 = 36.8\ \Omega)$ as a single linear slot array antenna. Furthermore, for the efficient design of the planar slot array antenna with low SLL in $yz$ cutting plane as well as input matching, it is necessary to decide the input impedance of a given linear slot array as a function of the coupling slot tilt angle and half-length.

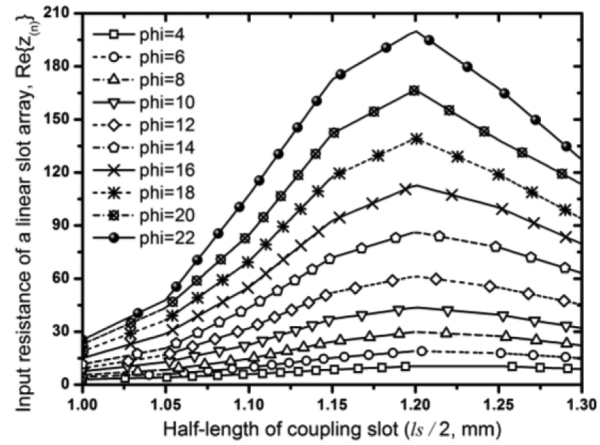


(a)

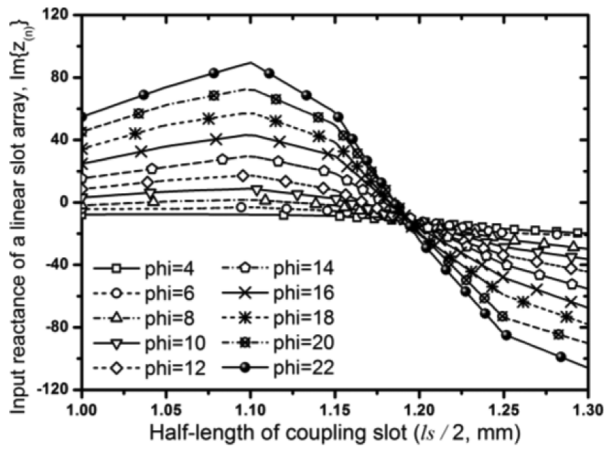


(b)

Fig. 7. The input impedance characteristics of a linear slot array as a function of the coupling slot length $(l_s)$ and the tilt angle $(p)$ when the width $(w_c)$ of the coupling slot is 0.5 mm. (a) Input resistance and (b) Input reactance.

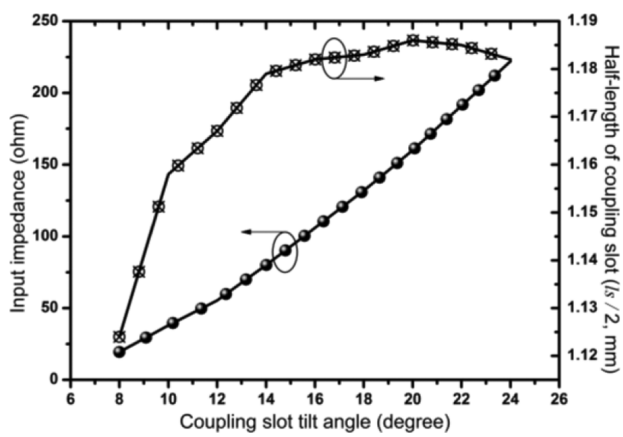


Fig. 8. The resonant condition for the series-to-series coupling slot which, is terminated with a linear slot array at port 3 and 4.

### *E. Coupling and Radiating Slot Arrangement for In-Phase Excitation*

There are two radiating slots adjacent to the coupling slot and they are separated with one quarter guided wavelength from the coupling slot location as shown in Fig. 9. In general, the coupled

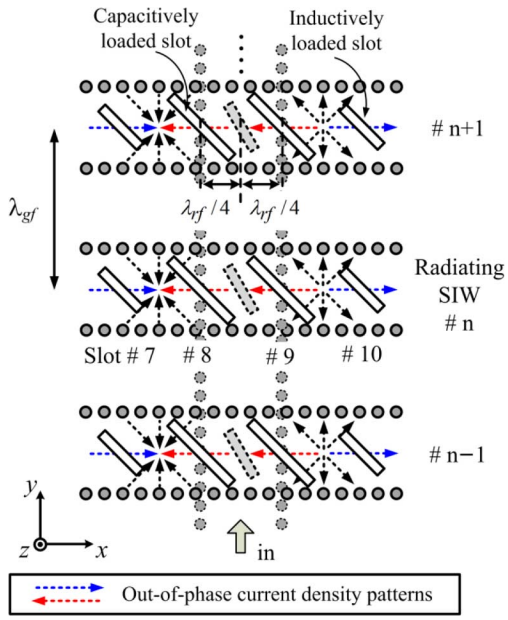


Fig. 9. The arrangement of the coupling and radiating slots for in-phase distribution with surface current density patterns.

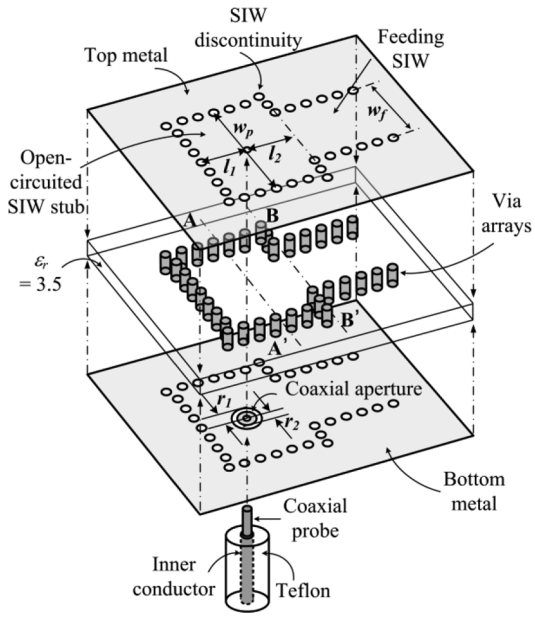


Fig. 10. The wideband stepped coax-to-SIW transition structure.

input signals toward the left $(-x)$ and right $(+x)$ sides of a radiating SIW are excited with the out-of-phase field distribution from the center of a series-to-series coupling slot. Furthermore, these coupled signals have alternative signs $(\pm x)$ due to the opposite direction of the propagation. As a result, the surface current density patterns on the upper metal plates of the radiating SIWs can generate, consequently, two adjacent radiating slots (slot #8 and #9) from a coupling slot and should have an equal length (i.e., inductive or capacitive slot) for the in-phase electric field distribution as depicted in Fig. 9. In addition, every coupling and radiating slot can be recursively arranged under the same orientation with the guided wavelength of a feeding SIW.

### *F. Wideband Coax-to-SIW Transition Design and Analysis*

The wideband coax-to-SIW transition is advantageous for the feeding network of antennas or circuits for which they are easily affected by the external electromagnetic coupling noises on account of their enclosed structure with the metal plates and via arrays. The coax-to-SIW transitions with an inductive matching via and asymmetric diaphragm have been invented for application to antenna feeding networks [15], [16]. In order to overcome the narrow bandwidth, the discontinuous width of the SIW for dual resonance was applied. This structure was previously suggested for the application of a transition between a metallic RWG and a post-wall waveguide [17].

As described in Fig. 10, in the bottom metal plate, the pattern of a coaxial aperture is formed with an outer $(r_1)$ and inner $(r_2)$ radius of 0.5 mm and 0.254 mm, respectively, for convenient and flexible matching. The open-ended rectangular cavity has a wider width $(w_p)$ than the width $(w_f)$ of a given feeding SIW. Therefore, a discontinuity is surely formed at the reference plane (BB') as depicted in Fig. 10. In addition, the open-circuited SIW stub consisting of a shorting via wall is located with the length of $l_1$ from the position of the coaxial probe that is the reference plane, AA'.

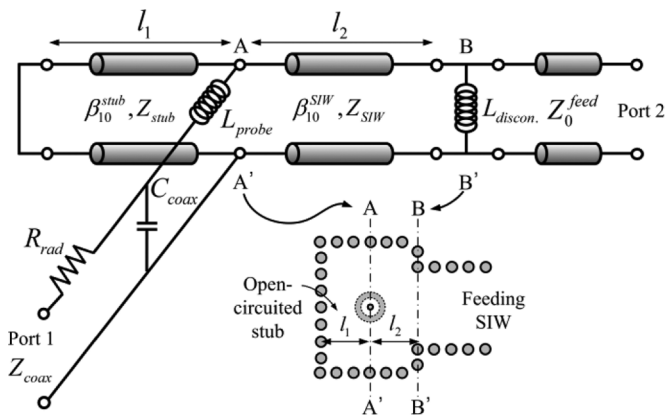


Fig. 11. The equivalent circuit model of the proposed wideband stepped coax-to-SIW transition.

The equivalent circuit of the proposed stepped coax-to-SIW transition is illustrated in Fig. 11. The coaxial probe can be modeled as the series connected resistance $(R_{rad})$ and inductance $(L_{\text{probe}})$, which represent the radiation loss to the internal bounded SIW medium and reactive near field of a coaxial probe, respectively [18]. The open-circuited SIW stub with the length and width of $l_1$ and $w_p$ are represented by the transmission line with a wave impedance of $Z_{\text{stub}}$ and a propagation constant of $\beta_{10}^{\text{stub}}$. In addition, the intermediate SIW line section between a coaxial probe (AA') and the discontinuity of the SIW (BB') has a length of $l_2$ with a wave impedance of $Z_{SIW}(= Z_{\text{stub}})$ as shown in Fig. 11. As the last part of the transition, the discontinuity at BB' can be modeled with the shunt inductance, $L_{discon}$, which can be controlled by the ratio of $w_f/w_p$ [19].

The validity of the proposed equivalent circuit model was confirmed with full-wave and circuit s-parameter simulation results with CST MWS and ADS [14], [20]. The dual resonant characteristic that occurred at 28.77 GHz and 37.31 GHz were found to be in good agreement with each other as depicted in

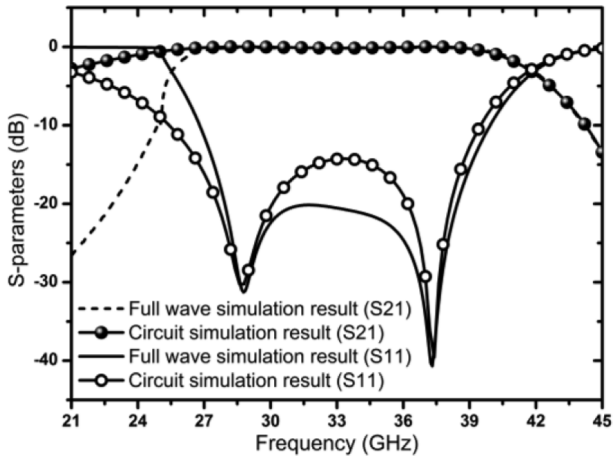


Fig. 12. S-parameter results of circuit and full-wave simulations for a single-ended stepped coax-to-SIW transition.

Fig. 12. It was also found that this dual resonance is independently generated by two sections of the transition. Specifically, the first and second resonant frequencies are controlled by the SIW discontinuity and open-circuited SIW stub, respectively. The electrical performances through the resonant frequency variation for the return loss with respect to the design parameters were verified. Fig. 13(a) shows that the first resonant frequency moves toward the lower bands as the width of a feeding SIW increases. This means that the transmission for the lower bands mainly relies on the cut-off frequency decided by the width of a feeding SIW. In addition, the second resonant frequency is dominantly controlled by the length of the open-circuited SIW stub as shown in Fig. 13(b). Likewise, the SIW stub can be seen as an open-circuit when the length of a stub is about a one-quarter guided wavelength. Therefore, the lower frequency component can be transferred with minimum reflection as the length of a SIW stub increases. Besides, the overall matching improvement of the transition is feasible with the coaxial aperture design parameter, $r_2$, as shown in Fig. 13(c). Eventually, a wideband transmission characteristic within a shielded structure can be realized. The design parameters and corresponding optimized values of the proposed planar slot array antenna including stepped coax-to-SIW transition are summarized in Table I.

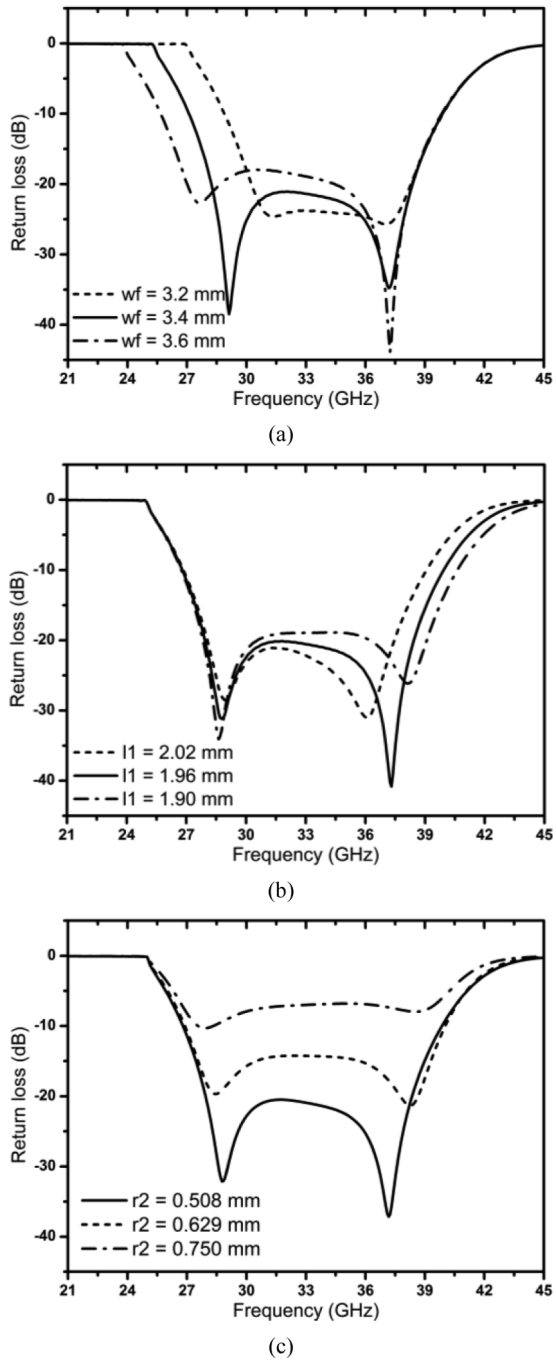


Fig. 13. The return loss variation according to the (a) the width of a feeding SIW ($w_f$), (b) the length of a open-circuited SIW stub ($l_1$), and (c) the radius of the coaxial aperture radius ($r_2$).

## IV. Electrical Performance

The electrical performances of the proposed planar slot array antenna designed following the procedures of Section III were analyzed with the results from the full-wave simulation and experimentation.

### *A. Uniform Electric Field Distribution*

To confirm the uniform electric field distributions on the antenna aperture, the amplitude and phase of the 45°-inclined electric field components were checked just above the aperture plane based on the design values summarized in Table I. The field uniformity for the radiating slots arrayed on the radiating SIW #1 was verified as depicted in Fig. 14(a). Specifically, the electric field distribution along the center line and 2 mm above the radiating SIW was verified. The sixteen peak values for the phase and amplitude were in the corresponding radiating slot locations along the $x$-axis and normalized to their maximum value. The difference between the maximum and minimum values of the phase distribution was 30° when their corresponding locations were $-21.7$ mm (slot #2) and 5.166 mm (slot #10), respectively. It was larger than that of the calculated result (19.07°) from Section III-B. It is conjectured that the self-impedances turn into active-impedances due to the mutual coupling affected by the adjacent radiating slots, as proved in preceding researches

TABLE I
DESIGN PARAMETERS AND OPTIMIZED VALUES

| | | | | |
|---|---|---|---|---|
| *Radiating SIW* | *Parameter* | $d$ | $d_x$ | $d_y$ |
| | *Value* | 0.4 | 3.34 | 6.88 |
| | *Parameter* | $h_u$ | $l_c$ | $s$ |
| | *Value* | 1.52 | 3.4 | 0.7 |
| | *Parameter* | $w$ | $w_s$ | $l_i$ |
| | *Value* | 3.44 | 0.4 | 2.32 |
| *Feeding SIW* | *Parameter* | $h_l$ | $h_b$ | $l_s$ |
| | *Value* | 0.75 | 0.101 | 1.1557 |
| | *Parameter* | $p$ | $w_f$ | $w_c$ |
| | *Value* | 9.87 | 3.38 | 0.5 |
| *Coax-to-SIW transition* | *Parameter* | $l_1$ | $l_2$ | $r_1$ |
| | *Value* | 1.96 | 2.15 | 0.5 |
| | *Parameter* | $r_2$ | $w_p$ | |
| | *Value* | 0.254 | 5.44 | |
| *Total structure* | *Parameter* | $L_l$ | $L_u$ | $W$ |
| | *Value* | 78 | 51.6 | 57.4 |

(Units: mm; degree for parameter '$p$' only)

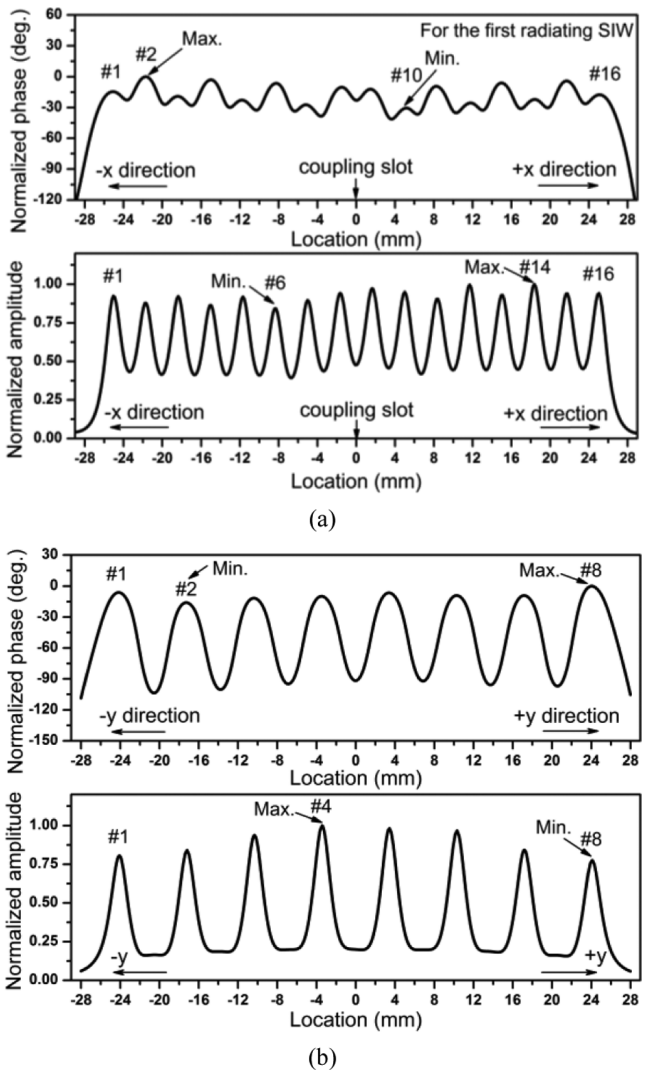


Fig. 14. The near aperture field distribution with respect to the phase and amplitude (a) for the radiating SIW #1 and (b) for 9th radiating elements (slot #9) of every radiating SIW.

[3], [4] for shunt slot array antennas. In addition, the uniformity of the normalized amplitude was obtained from the ratio

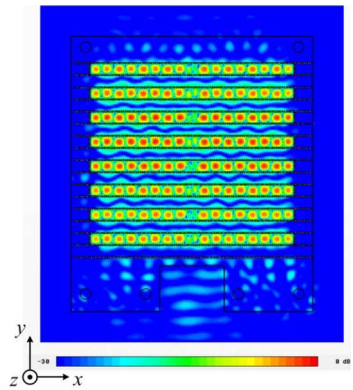


Fig. 15. The simulated aperture distribution with respect to the electric field amplitude.

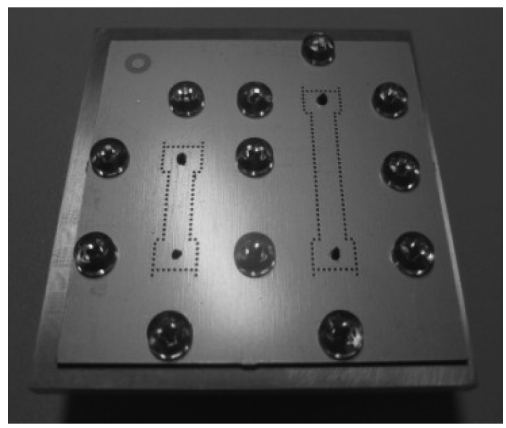

Fig. 16. The fabricated back-to-back stepped coax-to-SIW transition.

(Min./Max.) of 0.843 ($-1.48$ dB) when their maximum and minimum fields were generated by slot #14 and slot #6, respectively. Moreover, the uniformity for the $yz$ cutting plane was also evaluated (Fig. 14(b)). There were eight peak values, which originated from every 9th radiating element for each radiating SIW. The phase difference and amplitude uniformity were 15.86° and 0.775 ($-2.21$ dB), respectively. Even though every radiating SIW had identical design values for the alternating reactance slot pairs and series-to-series coupling slots, there were asymmetric properties for the phase and amplitude. Nevertheless, the acceptable uniform aperture field distribution was realized and verified with the full-wave simulation result (Fig. 15).

### B. Back-to-Back Coax-to-SIW Transition

The back-to-back transition was designed and fabricated as shown in Fig. 16. The Teflon and inner conductor were inserted into the hole of a metal housing and connected with a 2.92 mm connector. The fabricated PCB patterns were firmly adhered with a metal housing using plastic screws and shared a common ground without any air gaps between them. The experiment was done with an E8361A network analyzer from Agilent. The s-parameter results showed wide band-pass characteristics for the Ka-band (Fig. 17). The simulated bandwidth was 33.4% ranging from 27.347 to 38.314 GHz under the criteria of VSWR 1.5:1 whereas the measured bandwidth was 30.13% ranging from 27.8 to 37.66 GHz. In addition, the measured insertion

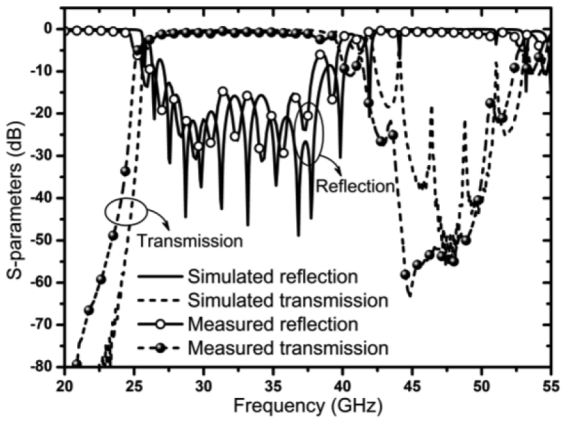


Fig. 17. The simulated and measured s-parameter results of the proposed coax-to-SIW transition.

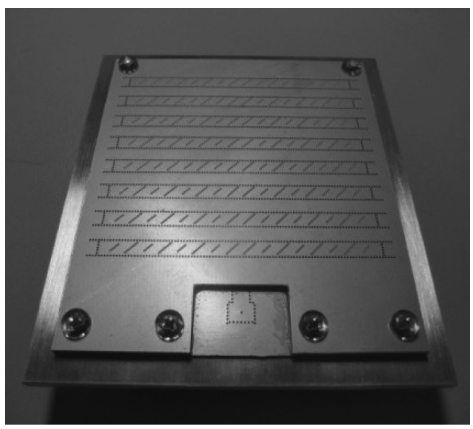

Fig. 18. The fabricated slot array antenna for 45° -inclined LP.

loss of the back-to-back transition was less than 1 dB within the pass-band frequency range.

### C. Reflection Coefficient, Gain, and Radiation Patterns

The proposed series slot array antenna was fabricated and set up for experiments to investigate the reflection coefficient, gain, and radiation patterns. A wideband transition imbedded planar slot array antenna was combined with metal housing to use a 50 Ω input port. The bottom metal plate of a feeding SIW shared a common ground with the metal housing (Fig. 18) for improved stability of electrical performance. The simulated and measured impedance bandwidths were from 34.46 to 35.34 GHz (2.52%) and from 33.86 to 34.85 GHz (2.88%) under the condition of less than VSWR 2:1, respectively. The center frequency shift was about 1.7% between the simulation and the measurement as described in Fig. 19 due to the etching error, which contributes to the variations in the self-impedances of the radiating slots.

The realized gain and radiation patterns for a 45°-inclined LP were proven in an anechoic chamber. The simulated and experimental maximum gains were 25.8 and 24.3 dBi at 35 and 34.8 GHz, respectively. Likewise, the aperture efficiency was 53.7% from a given aperture area of $57.4 \times 51.6$ mm and measured gain. The radiation patterns in $zx$ and $yz$ planes are depicted in Fig. 20. The simulated and experimental results were well matched each other. The simulated SLLs for each cutting

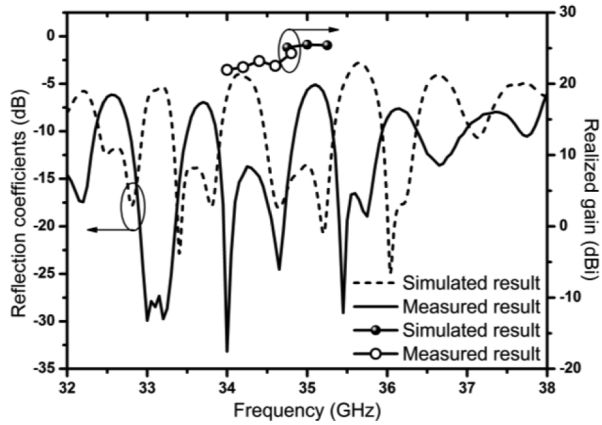


Fig. 19. The simulated and measured reflection coefficients and realized gain.

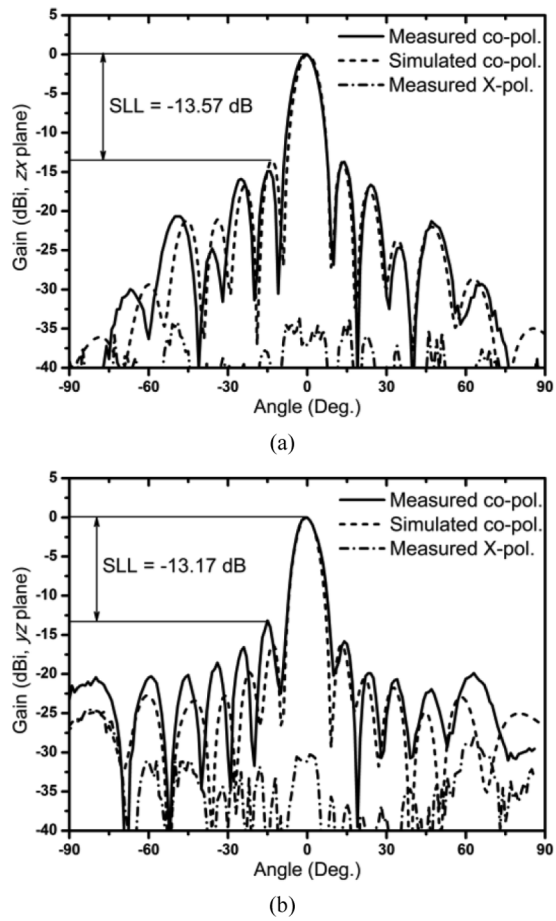


Fig. 20. Radiation patterns for (a) $zx$ plane and (b) $yz$ plane, respectively.

planes were $-13.6$ and $-16.2$ dB and the measured values were $-13.57$ and $-13.17$ dB, respectively. It was verified that a uniform field distribution was realized based on the measured SLLs despite their slight increase of about 3 dB. It was revealed that the proposed slot array antenna radiates purely 45°-inclined LP because the measured cross polarization discrimination (XPD) was less than $-30$ dB for all cutting planes. The measured electric performances of the proposed antenna as well as the half power beam width (HPBW) for each cutting plane are presented in Table II.

TABLE II
MEASURED ELECTRICAL PERFORMANCES

| *Bandwidth* | *HPBW* | | *Gain* |
|---|---|---|---|
| | *zx* | *yz* | |
| 2.88% | 8.2° | 7.9° | 24.3 dBi |
| *XPD* | *SLL* | | *Aperture efficiency* |
| | *zx* | *yz* | |
| -30.26 dB | -13.57 dB | -13.17 dB | 53.7% |

## V. CONCLUSIONS

A standing-wave-fed series slot array was proposed for a 45°-inclined LP in the Ka-band. All radiating and feeding lines were integrated in a multi-layered PCB with the SIW technique. Alternating reactance slot pairs with non-resonant slot lengths and equal slot spacing were adopted to implement impedance matching and uniform field distribution as well as side lobe suppression. The equivalent circuit models with the transmission line were presented and analyzed for the antenna components such as the linear slot array and total planar slot array antenna. Furthermore, the wideband stepped coax-to-SIW transition was also evaluated by an equivalent circuit model and verified from the circuit and full-wave simulation results. It was confirmed that the imbedded and enclosed transition helps the proposed antenna to radiate stable 45°-inclined LP without any distortion. The proposed antenna showed highly efficient electrical performances such as aperture efficiency and realized gain of 53.7% and 24.3 dBi, respectively, at 34.8 GHz with a XPD level of less than $-30$ dB. Furthermore, the measured SLLs for each cutting plane with $-13.57$ dB and $-13.17$ dB confirmed the uniform aperture field distribution. As a result, we expect that the lightweight and low costs features of a SIW slot array antenna with stable electrical performances can be designed with the proposed design method for millimeter-wave radiating systems.

## REFERENCES


[1] K. Hashimoto, J. Hirokawa, and M. Ando, "A post-wall waveguide center-feed parallel plate slot array antenna in the millimeter-wave band," *IEEE Trans. Antennas Propag.*, vol. 58, no. 11, pp. 3532–3538, Nov. 2010.

[2] K. Sakakibara, Y. Kimura, J. Hirokawa, and M. Ando, "A two-beam slotted leaky waveguide array for mobile reception of dual-polarization DBS," *IEEE Trans. Veh. Tech.*, vol. 48, no. 1, pp. 1–7, Jan. 1999.

[3] R. S. Elliott, "An improved design procedure for small arrays of shunt slots," *IEEE Trans. Antennas Propag.*, vol. AP-31, pp. 48–53, Jan. 1983.

[4] M. Orefice and R. S. Elliott, "Design of waveguide-fed series slot arrays," *IEE Proc.*, vol. 129, pp. 165–169, Aug. 1982.

[5] H. Oraizi and M. T. Noghani, "Design and optimization of waveguide-fed centered inclined slot arrays," *IEEE Trans. Antennas Propag.*, vol. 57, no. 12, pp. 3991–3995, Dec. 2009.

[6] J. Hirokawa and M. Ando, "45° linearly polarized post-wall waveguide-fed parallel-plate slot arrays," *IEE Proc.-Microw. Antennas Propag.*, vol. 147, no. 6, pp. 515–519, Dec. 2000.

[7] S. Park, Y. Okajima, J. Hirokawa, and M. Ando, "A slotted post-wall waveguide array with interdigital structure for 45° linear and dual polarization," *IEEE Trans. Antennas Propag.*, vol. 53, no. 9, pp. 2865–2871, 2005.

[8] A. Mizutani, K. Sakakibara, N. Kikuma, and H. Hirayama, "Grating lobe suppression of narrow-wall slotted hollow waveguide millimeter-wave planar antenna for arbitrarily linear polarization," *IEEE Trans. Antennas Propag.*, vol. 55, no. 2, pp. 313–320, Feb. 2007.

[9] F. Xu and K. Wu, "Guided-wave and leakage characteristics of substrate integrated waveguide," *IEEE Trans. Microwave Theory Tech.*, vol. 53, no. 1, pp. 66–73, Jan. 2005.

[10] D. Kim, W. Chung, C. Park, S. Lee, and S. Nam, "Design of a 45°-inclined SIW resonant series slot array antenna for Ka band," *IEEE Antennas Wireless Propag. Lett.*, vol. 10, pp. 318–321, 2011.

[11] D. Kim and S. Nam, "A Ka band planar slot array antenna for 45 degree linear polarization using substrate integrated waveguide," in *Proc. Eur. Conf. on Antennas and Propagation (EuCAP2011)*, Rome, Italy, Apr. 11–15, , pp. 2351–2353.

[12] J. C. Coetzee, J. Joubert, and D. A. McNamara, "Off-center-frequency analysis of a complete planar slotted-waveguide array consisting of subarray," *IEEE Trans. Antennas Propag.*, vol. 48, no. 11, pp. 1746–1755, Nov. 2000.

[13] G. Mazzarella and G. Montisci, "Wideband equivalent circuit of a centered-inclined waveguide slot coupler," *J. Electromagn. Waves Applicat.*, vol. 14, pp. 133–151, 2000.

[14] CST Microwave Studio (MWS) CST Corporation, 2010 [Online]. Available: http://www.cst.com

[15] T. Kai, Y. Katou, J. Hirokawa, M. Ando, H. Nakano, and Y. Hirachi, "A coaxial line to post-wall waveguide transition for a cost-effective transformer between a RF-device and a planar slot-array antenna in 60 GHz band," *IEICE Trans. Commun.*, vol. E89-B, no. 5, pp. 1646–1653, May 2006.

[16] D. Kim, J. W. Lee, T. K. Lee, and C. S. Cho, "Design of SIW cavity-backed circular-polarized antennas using two different feeding transitions," *IEEE Trans. Antennas Propag.*, vol. 59, no. 4, pp. 1398–1403, Apr. 2011.

[17] T. Kai, J. Hirokawa, and M. Ando, "A stepped post-wall waveguide with aperture interface to standard waveguide," in *IEEE AP-S Int. Symp. Dig.*, 2004, pp. 1527–1530.

[18] G. K. C. Kwan and N. K. Das, "Excitation of a parallel-plate dielectric waveguide using a coaxial probe-basic characteristics and experiments," *IEEE Trans. Microwave Theory Tech.*, vol. 50, no. 6, pp. 1609–1619, Jun. 2002.

[19] N. Marcuvitz, *Waveguide Handbook*. New York: McGraw-Hill, 1951, pp. 296–298.

[20] Agilent technologies Advanced Design System (ADS), 2009 [Online]. Available: http://www.agilent.com


**Dong-yeon Kim** received the B.S. and M.S. degrees in electronics, telecommunications and computer engineering from Korea Aerospace University, Goyang, in 2007 and 2009, respectively. He is now working toward the Ph.D. degree in Seoul National University, Seoul, Korea.

His research interests include microwave and millimeter-wave antenna design and analysis, EMI/EMC analysis on PCBs.

**Woo-Sung Chung** received the B.S. and M.S. degrees in electronic engineering in 2002 and 2006, respectively, from Hongik University, Seoul, Korea.

From 2002 to 2004, he was a researcher at HYUNDAI Rotem R&D Center, Uiwang, Korea. From 2006 to 2009, he worked for Agency for Defense Development (ADD), Deajeon, Korea. Since 2009, he has been with LIG Nex1 ISR R&D Lab, Yongin, Korea. His current research interests include analysis of antenna and radome.

**Chang-Hyun Park** received the B.S. and M.S. in electronic engineering in 1997 and 1999, respectively, from SungKyunKwan University, Korea.

Since 1999, he has been with LIG Nex1 ISR R&D Lab, Yongin, Korea. His current research interests include design and analysis of antenna and radome, and RF senor system development.

**Sang-Joo Lee** received the B.S. and M.S. degrees in electronic engineering in 1986 and 1988, respectively, from Hongik University, Seoul, Korea.

Since 1990, he has been with LIG Nex1 ISR R&D Lab, Yongin, Korea, where he is now a team leader. His current research interests include antenna, microwave wave circuit, radar, RF senor system development.

**Sangwook Nam** (S'87–M'88) received the B.S. degree from Seoul National University, Seoul, Korea, in 1981, the M.S. degree from the Korea Advanced Institute of Science and Technology (KAIST), in 1983, and the Ph.D. degree from the University of Texas at Austin, in 1989, all in electronics/electrical engineering.

From 1983 to 1986, he was a Researcher with the Gold Star Central Research Laboratory, Seoul, Korea. Since 1990, he has been with Seoul National University, where he is currently a Professor in the School of Electrical Engineering. His research interests include analysis/design of electromagnetic (EM) structures, antennas, and microwave active/passive circuits.